Fiber optic pressure sensing with conforming elastomers

Li-Yang Shao,[1,2,*] Qi Jiang,[2] and Jacques Albert[2]

[1]Institute of Optoelectronic Technology, China Jiliang University, Hangzhou 310018, China

[2]Department of Electronics, Carleton University, Ottawa, Ontario K1S 5B6, Canada

*Corresponding author: liyangshao@gmail.com

A novel pressure sensing scheme based on the effect of a conforming elastomer material on the transmission spectrum of tilted fiber Bragg gratings is presented. Lateral pressure on the elastomer increases its contact angle around the circumference of the fiber and strongly perturbs the optical transmission of the grating. Using an elastomer with a Young's modulus of 20 MPa, a Poisson ratio of 0.48, and a refractive index of 1.42, the sensor reacts monotonically to pressures from 0 to 50 kPa (and linearly from 0 to 15 kPa), with a standard deviation of 0.25 kPa and maximum error of 0.5 kPa. The data are extracted from the optical transmission spectrum using Fourier analysis and we show that this technique makes the response of the sensor independent of temperature, with a maximum error of 2% between 25 °C and 75 °C. Finally, other pressure ranges can be reached by using conforming materials with different modulii or applying the pressure at different orientations.   © 2010 Optical Society of America

OCIS codes: 060.2340, 060.2370, 050.2770.

1. Introduction

The resonance wavelengths of the transmission or reflection spectrum of in-fiber Bragg gratings (FBGs) are widely used for measuring structural deformations, but they work best for longitudinal strain; most sensor systems use multiple gratings to measure more complex deformations. Recently, there has been increasing interest in sensing transverse strain (in a host material) or lateral pressure directly applied on the fiber [1,2]. Because of the high value of the Young's modulus of the fiber (approximately 70 GPa), lateral (or even hydrostatic pressure) has little effect on the Bragg wavelength of fiber gratings. However, external transverse pressure creates additional birefringence in the fiber and leads to splitting of FBG resonances in two orthogonal polarization modes. To enhance this sensitivity, FBGs have been fabricated in high birefringence or microstructured fibers [3], with the added benefit of a lower "effective" Young's modulus in the latter case because of the air holes in the fiber. In most of these cases, only Hertzian contact (i.e., single point or line contact between two hard and undeformed materials, glass and metal, for instance) is investigated. In the Hertzian contact zone, contacting objects experience extremely small deformations compared with the overall dimensions and the induced-birefringence is a linear function of the applied transverse pressure, with little room for optimizing the response to various pressure ranges.

Unfortunately, many applications deal with conforming contact between materials with elastic modulii (several tens of megapascals) that are orders of magnitude lower than that of fibers. For example, researchers have investigated the mechanical characteristics of different wheelchair seat cushions used for patients with spinal cord injury in terms of pressure distribution and contact surface at the user–cushion interface [4]. In industrial applications, contact pressure distribution at hand–handle interface has been mapped to investigate the ergonomic efficiency of handles with different sizes [5]. There are also several

biomechanics applications where conforming contact must be dealt with: contact area and pressure distribution are often measured in artificial joints, such as knee, hip, and tibiofemoral bones, which is very important in predicting joint degradation mechanisms and prosthetic implant wear, providing biomechanical rationales for preoperative planning and post-operative rehabilitation [6,7]. In a recent report, the use of an FBG written in a birefringent fiber has been proposed to measure the conforming contact pressure (independent of the modulii of contacting materials) by monitoring the spectral separation of Bragg wavelengths that correspond to the slow and fast axes of the fiber [8]. However, this introduces another operational problem: the difficulty to align the direction of contact pressure along the fast or slow axis of the birefringent fiber.

In this paper, we demonstrate a simple alternative contact pressure sensor incorporating a tilted FBG (TFBG) in a standard single mode fiber compressed between two conforming elastomer layers. The TFBG couples light from the core to a multitude of cladding modes over a wide spectral range [9] and the applied pressure increases the contact area between the surface of the cladding of the optical fiber and the conforming elastomer. When the contact area with a high refractive index and lossy elastomer increases, the cladding modes become lossy and, as a consequence, the visibility of high order cladding mode optical transmission resonances decreases with applied pressure. Applying a fast Fourier transform (FFT) analysis of a suitable region of the transmission spectrum provides a direct measure of the visibility and, hence, of the pressure [10]. The FFT approach has the advantage of being immune to power fluctuations from the light source or fiber link, and also to the absolute wavelengths of the cladding mode resonances (at least for absolute wavelength changes that are small compared to the spectral range used). The latter feature makes our device independent of temperature, as will be demonstrated below over the range from 25 °C to 75 °C. Finally, although the proposed sensor is also orientation dependent, it does not need to be aligned very precisely to the direction of the applied transverse load (unlike the birefringent FBG sensor). The additional advantage is that other pressure ranges can be reached by using conforming materials with different modulii or applying the pressure at different orientations.

2. Sensing Principle

As a basis for our proposed sensor, TFBGs represent a natural choice because of the ease and control with which they couple to cladding modes that can be used to detect changes in the environment of the sensor. The Bragg wavelength and cladding mode resonance wavelengths λ_{Bragg} and λ_{clad}^i of TFBGs are determined by the following phase matching condition [11]:

$$\lambda_{\text{Bragg}} = 2N_{\text{eff}}(\text{core}) * \Lambda / \cos(\theta), \quad (1a)$$

$$\lambda_{\text{clad}}^i = (N_{\text{eff}}(\text{core}) + N_{\text{eff}}^i(\text{clad})) * \Lambda / \cos(\theta), \quad (1b)$$

where Λ is the grating period, θ is the tilt angle of the grating planes, and $N_{\text{eff}}(\text{core})$ and $N_{\text{eff}}^i(\text{clad})$ are the effective index of the core mode and the ith order cladding mode measured at the resonance wavelengths. When the fiber section that contains the TFBG is located in air, the index contrast with the cladding is large and so is the fiber diameter (125 μm), meaning that hundreds of cladding modes can be guided, resulting in a TFBG transmission spectrum with an equivalent number of resonances. The amplitudes of the resonances depend on the strength of the index modulation that gives rise to the grating, the length of the grating, and on the tilt angle. When the refractive index of the medium surrounding the fiber increases, those modes with effective indices that are lower than the surrounding index become radiative and, hence, lossy. As shown in Ref. [12], this has the effect of decreasing strongly the amplitudes of the transmission resonances of the modes that have become radiative. A similar effect occurs when the surrounding medium is also lossy, but with the significant difference that, in such case, the amplitudes of ALL resonances decrease. In the contact pressure experiment, the elastomer is initially in Hertzian contact with the fiber and the fiber environment is mostly air. However, with increasing pressure, and depending on the magnitude of its elastic modulus, the elastomer gradually wraps around the surface of the fiber and, hence, modifies the propagation characteristics of the cladding modes. Between the two extreme cases (fiber in air and fiber completely surrounded by elastomer), our main finding here is that the amount of perturbation of the cladding mode resonances is in direct relation with the contact angle between the optical fiber and the conforming elastomer. This is our pressure sensing mechanism.

Figure 1(a) shows the schematic diagram of the configuration we use to apply lateral pressure in the experiment. The TFBG was placed between two elastomer layers (20 mm wide, 20 mm long, and 2 mm thick), while a segment of stripped single mode fiber with identical size was placed 1 cm away from the sensing fiber to ensure that the force is applied diametrically on the fiber. The elastomer layers and optical fibers were subjected to transverse pressure between two glass slides with smooth surfaces (20 mm × 20 mm). Transverse pressure was applied by compressing a steel cylinder (diameter 16 mm) on the top glass slide with a micrometer screw and measured accurately by a precalibrated load cell (Lloyd Instrument, Inc.). Figure 1(b) illustrates the geometry of the contact between the optical fiber and the conforming elastomer. For the case of small deformations (contact angle ≤ 5°), we can employ the following formula to determine the contact angle θ as a function of transverse pressure or load F [13]:
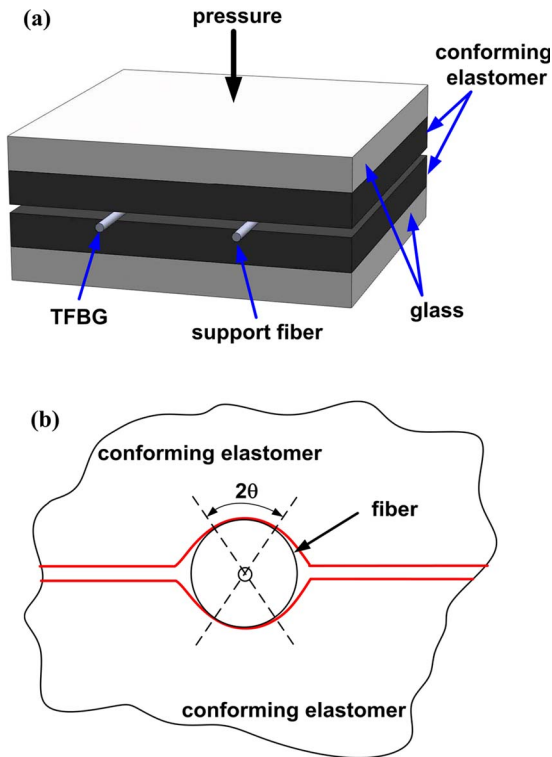
Fig. 1. (Color online) Schematic diagram of (a) the pressure applying configuration and (b) the geometry of contact between the optical fiber and the conforming elastomer.

$$\frac{E^*\Delta R}{F/l} = \frac{(\alpha-1)(\log[\tan^2(\theta/2)+1]+2\tan^4(\theta/2))+2}{\pi(1+\alpha)(\tan^2(\theta/2)+1)\tan^2(\theta/2)}$$
$$- \frac{4\beta}{\pi(1+\alpha)}, \qquad (2)$$

where E^* is the plane strain Young's modulus of the fiber, ΔR is the radius difference of elastomer and fiber, and l is the length of fiber between two elastomer layers. α and β are material constants that are functions of the Young's modulii and Poisson ratios. The ratios η and ς are variables used in the calculation of α and β:

$$\eta = E_1^*/E_2^*, \qquad (3a)$$

$$\varsigma = (1-v_1^*) - \eta(1-v_2^*), \qquad (3b)$$

where $\nu_{(1,2)}^*$ are the plane strain Poisson ratios of the fiber and the conforming elastomer. Then α and β can be calculated by

$$\alpha = \frac{1-\eta}{1+\eta}, \qquad (4a)$$

$$\beta = \frac{1}{2}\frac{\varsigma}{1+\eta}. \qquad (4b)$$

The Young's modulus and Poisson ratio of the optical fiber were specified at 70 GPa and 0.17, respectively. The conforming elastomer we use is a silicone rubber,

whose Young's modulus and Poisson ratio were 20 MPa and 0.48. The predicted contact angles are plotted in Fig. 2 with applied transverse load changes. Although the model cannot be applied to the largest deformations of the elastomer, we will be able to compare qualitatively the conforming contact behavior with the experimental results at small contact angles.

3. Experiments

Corning SMF-28 fiber was used to fabricate the TFBGs in the experiment. The fiber was soaked in a hydrogen chamber for 12 days at 2500 psi and room temperature of 25 °C to improve its photosensitivity. A 1 cm long TFBG with a tilt angle of 10° was inscribed in the hydrogen-loaded fibers using a pulsed KrF excimer laser and the phase mask technique. To excite high order cladding modes spectrally located in the vicinity of 1550 nm, the period of the phase mask was chosen to be 1106.5 nm. The resulting Bragg wavelength (spectral resonance corresponding to the core mode reflection) of the TFBG is 1602.36 nm. A broadband light source and optical spectrum analyzer were used to measure the spectrum evolution of the sensing TFBG.

The transverse load force F was applied from 0 to 20 N. The corresponding contact pressure can be easily calculated by $P = F/A$, where A is the area of the device under pressure (4×10^{-4} m^2). This corresponds to a pressure range of 0 to 50 kPa. Since the pressure range can be adjusted simply by changing the size of the plates, our results will be expressed using load units in the following. To investigate the orientation dependent property, we have also adjusted the direction for applying pressure on the fiber. The orientation of 0° is defined by the direction at which the sensor has maximum sensitivity. The responses at another two orientations, 45° and 90°, are recorded referring to the direction of 0°. Figure 3(a) shows the spectrum evolution of the TFBG when the transverse load changes at the orientation of 0°. While the spectrum at zero load is identical to the spectrum of the grating in air (as it should be), the effect of increasing the load does not correspond to the
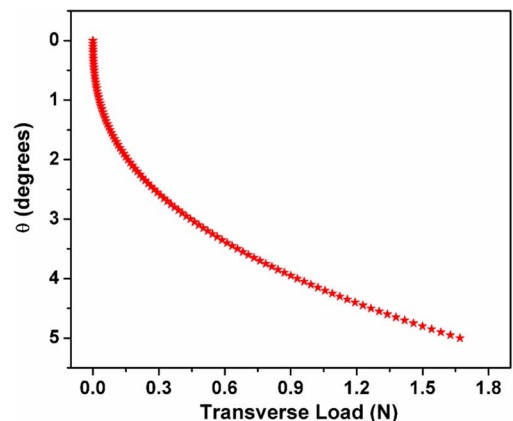

Fig. 2. (Color online) Simulated contact angles between fiber and conforming elastomer versus applied transverse loads.

spectral changes that are expected when the surrounding refractive index increases [12]. Instead, we observe a decrease in the amplitude of the resonances that can be associated with an effective increase of the loss due to the surrounding medium. The net result is that the visibility of the fringe pattern in the spectrum decreases monotonically with the transverse load. In order to quantify the fringe visibility response, a band from 1520 to 1585 nm was selected for the FFT analysis. Figure 3(b) depicts the results of the FFT analysis (using a Hanning windowing procedure) of the wavelength data in Fig. 3(a). Then Fig. 4 illustrates how the peak amplitude (of the dominant frequency around 0.8 nm^{-1}) changes under different transverse loads at three orientations (0°, 45°, 90°). In Fig. 4, the black dashed curve is a third-order polynomial regression of the measured peak amplitude data (at the orientation of 0°) with an R-square value of 0.995 and standard deviation of ±0.1 N (equals to 0.25 kPa). And there is a quasi-linear response from 0 to 8 N (equals to 0–20 kPa) with a sensitivity of 125 arbitrary units/N. Measurements at the orientation of 0° were repeated 30 times and the variation of the results is indicated by the size of the error bars. The maximum measurement
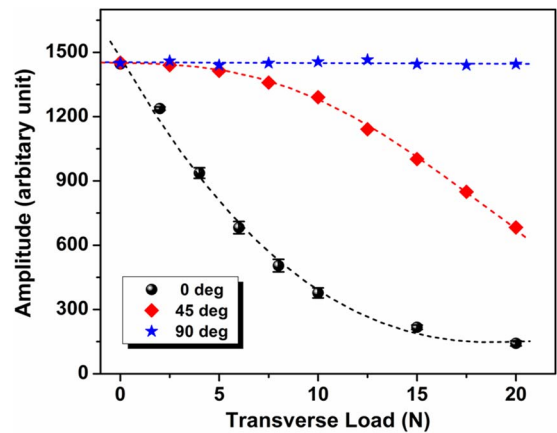
Fig. 4. (Color online) Peak amplitude of the dominant frequency around 0.8 nm^{-1} versus transverse load at three orientations (0°, 45°, 90°).

deviation (at 8 N) is ±0.2 N (equals to 0.5 kPa). The shape of the response curve reflects the facts that the process is self-limiting (once the cladding mode field in the circumference of the fiber is completely surrounded, increasing the pressure further will not increase the losses around the cladding) and that theory predicts that the contact angle does not increase linearly with transverse load (the nonlinearity of the response has the same qualitative shape as seen on Fig. 2). Rotating the fiber by 90° away from the optimum orientation makes the sensor nearly independent of the transverse load while, for an orientation of 45° (in between these two extremes), the peak amplitude also decreases monotonically with the applied transverse load but the sensitivity is much smaller than for 0°. These results undoubtedly stem from the specific mode coupling properties of the TFBG with regard to the orientation of the tilt plane, an effect already observed and utilized for a vector inclinometer based on a bent TFBG [14] and for a polarization selective surface plasmon coupler [15]. In the present case, the extreme sensitivities observed at 0° and 90° must correspond to orientations that are parallel and perpendicular to the tilt plane of the grating and result from a large difference in the cladding mode field distributions around the circumference. It appears that, for the 90° case, the symmetries of the cladding modes excited by the TFBG have minima in the direction of the contact points of the elastomer and, hence, do not feel its influence until the pressure pushes the elastomer almost fully around the circumference. An interesting aspect of this feature is that the dependence of the sensitivity on orientation provides an additional degree of freedom (beyond the elastic modulus of the elastomer) to tune the pressure measurement range of a given TFBG.

Finally, we have studied the cross sensitivity of the pressure response to temperature by imposing a constant load of 3.8 N on a device in contact with a hot plate. Figure 5 shows the FFT analysis of the TFBG spectra (in the same wavelength band) as a function of device temperature. Over the range from 25 °C to 75 °C, the peak amplitude of the FFT changes by
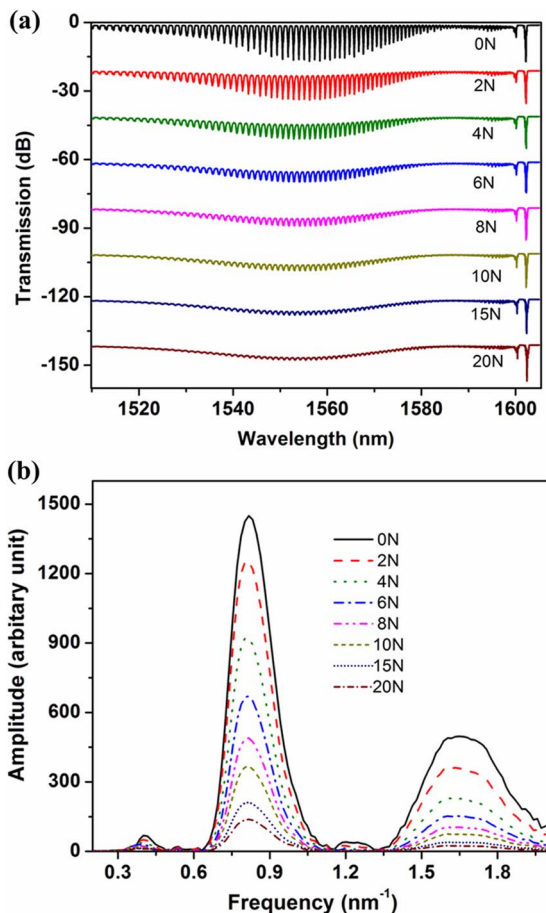

Fig. 3. (Color online) (a) Evolution of the optical spectra of a 10° TFBG with transverse load changes. (b) Corresponding FFT spectra extracted from the wavelength band in the range of 1520 to 1585 nm (at an orientation of 0°; see text for details).

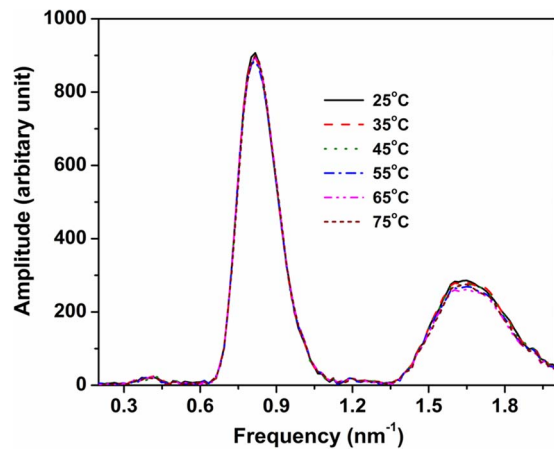Fig. 5. (Color online) FFT analysis of a 10° TFBG with temperature changes in the range of 25 °C to 75 °C (under constant contact load of 3.8 N and orientation of 0°).

only 2%. This corresponds to a temperature-induced measurement error of the order of 0.1 N for that load. If the temperature cross sensitivity must be decreased further, the TFBG possesses a very accurate local thermometer (the core mode resonance wavelength is by definition impervious to changes outside the cladding and provides a very accurate measure of the local temperature) that can be used to correct the response after proper calibration of the sensor.

4. Conclusion

In conclusion, by placing a TFBG between two materials that can deform around it when pressure is applied to the whole structure, it is possible to augment considerably the range of pressures that can be sensed with the relatively rigid fiber device. The structure is very simple to fabricate and the data extraction scheme (FFT analysis) is also straightforward and robust. We obtain an orientation-dependent response when the conforming elastomer gradually surrounds the fiber diameter. We have shown precise, reproducible pressure readings over the range from 0 to 50 kPa with maximum errors, statistical deviations, and temperature cross sensitivity of the order of 1 kPa at the orientation of 0°. While it was not demonstrated here, using deformable materials with different elastic modulii will obviously change the range of pressures that can be detected. We also demonstrated that the response of the device does not change for small temperature variations (i.e., small enough to avoid drastic changes in the optical properties of the conforming materials). By comparison with alternative FBG sensing technologies, which rely mostly on packaged FBGs under tension, with a mechanical transduction mechanism to convert pressure into a change of the tension on the FBG, our device is significantly simpler to implement, is less temperature sensitive, and is potentially much more reliable, as the glass fiber is inherently stronger in compression than in tension.

References

1. C. M. Lawrence, D. V. Nelson, E. Udd, and T. Bennett, "A fiber optic sensor for transverse strain measurement," Exp. Mech. **39**, 202–209 (1999).
2. M. Silva-Lopez, C. Li, W. N. MacPherson, A. J. Moore, J. S. Barton, J. D. C. Jones, D. Zhao, L. Zhang, and I. Bennion, "Differential birefringence in multicore fiber Bragg gratings under transverse stress," Opt. Lett. **29**, 2225–2227 (2004).
3. H.-M. Kim, T.-H. Kim, B. Kim, and Y. Chung, "Enhanced transverse load sensitivity by using a highly birefringent photonic crystal fiber with larger air holes on one axis," Appl. Opt. **49**, 3841–3845 (2010).
4. A. Gil-Agudo, A. De la Peña-González, A. Del Ama-Espinosa, E. Pérez-Rizo, E. Díaz-Domínguez, and A. Sánchez-Ramos, "Comparative study of pressure distribution at the user-cushion interface with different cushions in a population with spinal cord injury," Clin. Biomech. **24**, 558–563 (2009).
5. Y. Aldien, D. Welcome, S. Rakheja, R. Dong, and P. E. Boileau, "Contact pressure distribution at hand-handle interface: role of hand forces and handle size," Int. J. Ind. Ergonom. **35**, 267–286 (2005).
6. D. R. Sparks, D. P. Beason, B. S. Etheridge, J. E. Alonso, and A. W. Eberhardt, "Contact pressures in the flexed hip joint during lateral trochanteric loading," J. Orthop. Res. **23**, 359–366 (2005).
7. S. Matsuda, T. Ishinishi, S. E. White, and L. A. Whiteside, "Patellofemoral joint after total knee arthroplasty: effect on contact area and contact stress," J. Arthroplasty **12**, 790–797 (1997).
8. C. R. Dennison and P. M. Wild, "Sensitivity of Bragg gratings in birefringent optical fiber to transverse compression between conforming materials," Appl. Opt. **49**, 2250–2261 (2010).
9. L.-Y. Shao, Y. Shevchenko, and J. Albert, "Intrinsic temperature sensitivity of tilted fiber Bragg grating based surface plasmon resonance sensors," Opt. Express **18**, 11464–11471 (2010).
10. S. Maguis, G. Laffont, P. Ferdinand, B. Carbonnier, K. Kham, T. Mekhalif, and M.-C. Millot, "Biofunctionalized tilted fiber Bragg Gratings for label-free immunosensing," Opt. Express **16**, 19049–19062 (2008).
11. T. Erdogan, "Cladding-mode resonances in short- and long-period fiber grating filters," J. Opt. Soc. Am. A **14**, 1760–1773 (1997).
12. Y.-P. Miao, B. Liu, and Q.-D. Zhao, "Refractive index sensor based on measuring the transmission power of tilted fiber Bragg grating," Opt. Fiber Technol. **15**, 233–236 (2009).
13. M. Ciavarella and P. Decuzzi, "The state of stress induced by plane frictionless cylindrical contact. II. The general case (elastic dissimilarity)," Int. J. Solids Struct. **38**, 4525–4533 (2001).
14. L.-Y. Shao and J. Albert, "Compact fiber-optic vector inclinometer," Opt. Lett. **35**, 1034–1036 (2010).
15. Y. Shevchenko, C. Chen, M. A. Dakka, and J. Albert, "Polarization-selective grating excitation of plasmons in cylindrical optical fibers," Opt. Lett. **35**, 637–639 (2010).